

# Adaptive Fuzzy Wavelet Neural Network Control for a Class of Nonlinear Systems Using Sliding-Mode Approach

Chun-Fei Hsu<sup>1\*</sup> Chien-Jung Chiu<sup>2</sup> Chih-Hu Wang<sup>1</sup> and Jang-Zern Tsai<sup>2</sup>

<sup>1</sup>Department of Electrical Engineering, Chung Hua University, Hsinchu 300, Taiwan, Republic of China

E-mail: fei@chu.edu.tw; mikewang@chu.edu.tw

<sup>2</sup>Department of Electrical Engineering, National Central University, Jung-Li 320, Taiwan, Republic of China

E-mail: intel@ms63.hinet.net; jztsai@ee.ncu.edu.tw

---

**Abstract:** In this paper, an adaptive fuzzy wavelet neural network control (AFWNNC) system composed of a neural controller and a robust compensator is proposed. The neural controller using a fuzzy wavelet neural network (FWNN) is designed to approximate an ideal controller, and the robust compensator is designed to ensure system stable. In many previous published papers, to ensure the stability of the intelligent control system, a switching compensator is designed to dispel the approximation error introduced by the neural controller. However, the switching compensator usually causes chattering phenomena. The proposed robust compensator is designed to eliminate the approximation error without occurring chattering phenomena. Moreover, a proportional-integral-derivative (PID) type adaptation tuning mechanism is derived to speed up the convergence of the tracking error and controller parameters. Finally, the proposed AFWNNC system is applied to a chaotic system and a DC motor. The simulation and experimental results verify the system stabilization, favorable tracking performance and no chattering phenomena can be achieved by the proposed AFWNNC system.

**Keywords:** Adaptive control, neural control, wavelet neural network, Lyapunov stability, chaotic system, DC motor.

---

## 1. INTRODUCTION

Neural network technology is an effective tool for dealing with complex nonlinear processes that are characterized with ill-defined and uncertain factors. The key factors for the use of neural networks in the control field are the properties that they have such as: learning and generalization abilities, nonlinear mapping, parallelism of computation, and vitality (Lin and Lee, 1996). Several adaptive neural network controllers have been successfully applied to solve the problem of identification and control for the uncertain nonlinear systems (Lin, 2005; Tang *et al.*, 2006; Wang *et al.*, 2008; Hsu, 2009). These approaches hinted the neural networks as a “black box”. It means neural networks can approximate a continuous function arbitrarily closely over a compact set. The basic issue of the adaptive neural network control provides online learning algorithms that don’t require preliminary off-line tuning. Some online learning algorithms are based on the Lyapunov stability theorem and some online learning algorithms are based on the gradient decent method.

For solving the majority of approximation problems, the neural networks require a large number of neurons. Furthermore, the neural networks may get stuck on a local minimum of the error surface, and the network convergence rate is generally slow. A suitable approach for overcoming these disadvantages is the use wavelet functions in the network structure to construct the wavelet neural network (WNN) (Zhang, 1997; Billings and Wei, 2005; Chauhan *et*

*al.*, 2009; Lin *et al.*, 2009). The wavelet function is a waveform that has limited duration and an average value of zero. Then, the WNN has a nonlinear regression structure that uses localized basis functions in the hidden layer to achieve the desired input-output mapping. The integration of the localization properties of wavelets and the learning abilities of neural network result in the advantages of WNN over neural network for complex nonlinear system modelling (Billings and Wei, 2005; Lin *et al.*, 2009). There has been considerable interest in exploring the applications of the WNN to deal with the non-linearity and uncertainty of control problems (Sousa *et al.*, 2002; Lin *et al.*, 2006 and 2009; Hsu *et al.*, 2006 and 2009; Khan and Rahman, 2008). To achieve better learning performance, Ho *et al.* (2001) have proposed a fuzzy wavelet neural network (FWNN) based on multi-resolution analysis of wavelet transforms and fuzzy concepts. The goal of the introduction of fuzzy model into WNN is to improve function approximation accuracy. Based on this advantage, several published papers used the FWNN to deal with the uncertain nonlinear systems (Lin, 2006 and 2009; Zekri *et al.*, 2008).

Since the number of hidden neurons in the neural network is finite for the real-time practical applications, the approximation error introduced by the neural network is inevitable. To ensure the system stability, a switching compensator was designed to dispel the approximation error. However, the switching compensator will cause chattering

phenomena to wear the bearing mechanism (Lin and Hsu, 2004). To reduce the chattering phenomenon, the sign function in compensator can be replaced by a saturation function (Lin and Hsu, 2004). However, there is a trade off problem between chattering and control accuracy rises. Some researchers using a fuzzy system to estimate the approximation error bound; however, the fuzzy rules should be pre-constructed by time-consuming trial-and-error tuning procedure (Lin *et al.*, 2005).

Moreover, though these FWNN-based adaptive neural network control systems (Lin, 2006 and 2009; Zekri *et al.*, 2008) can guarantee the system's stability, the convergence of the controller parameters and tracking errors may be slow. If the learning-rate parameters are too small, the convergence of the tracking error and controller parameters can be easily guaranteed but the convergence speed is very slow. If the learning-rate parameters are too large, the parameter adaptation laws may become unstable. To solve this problem, a variable learning rate is determined (Lin and Peng, 2004; Lin *et al.*, 2007). Lin and Peng (2004) used a discrete-type Lyapunov function to determine the learning-rate parameters of the adaptation laws. However, the exact calculation of the Jacobian term of the system cannot be determined due to the unknown control dynamics. Lin *et al.* (2007) used a genetic algorithm to determine the learning-rate parameters of the adaptation laws; however, the computation loading is heavy.

In this paper, an adaptive fuzzy wavelet neural network control (AFWNNC) system composed of a neural controller and a robust compensator is proposed. The neural controller uses a FWNN to approximate an ideal controller; and the robust compensator is utilized to eliminate the approximation error between neural controller and ideal controller without occurring chattering phenomena. To speed up the convergence of the tracking error and the controller parameters, this paper derives a proportional-integral-derivative (PID) type adaptation law based on the Lyapunov stability theory, thus not only the system stability can be guaranteed but also the convergence can be speeded up. Finally, the proposed AFWNNC system is applied to a chaotic system and a DC motor. The simulation and experimental results show the high tracking performance and no chattering phenomena can be achieved by the proposed AFWNNC system.

## 2. DESCRIPTION OF FWNN

Assume there are  $m$  rules in FWNN can be described as (Zekri *et al.*, 2008; Lin, 2009)

Rule  $i$ : If  $z_1$  is  $A_1^i$  ... and  $z_n$  is  $A_n^i$ , Then  $\Xi$  is  $\alpha_i \psi_i(\mathbf{z})$  (1) where  $\mathbf{z} = [z_1, z_2, \dots, z_n]^T$  and  $\Xi$  are the input vector and output variable of FWNN, respectively;  $A_j^i$  are the linguistic terms characterized by their corresponding fuzzy membership functions of the fuzzy sets; and  $\alpha_i \psi_i(\mathbf{z})$  is the output weight.

$\psi_i(\mathbf{z}) = \prod_{k=1}^n (1 - \omega_{ki}^2 z_k^2)$  is defined as the "Mexican hat" mother wavelet function. The FWNN performs the mappings according to

$$\Xi = \sum_{i=1}^m \alpha_i \psi_i(\mathbf{z}) \phi_i(\boldsymbol{\sigma}_i, \|\mathbf{z} - \mathbf{c}_i\|) \quad (2)$$

where  $\boldsymbol{\sigma}_i = [\sigma_{1i} \sigma_{2i} \dots \sigma_{ni}]$  and  $\mathbf{c}_i = [c_{1i} c_{2i} \dots c_{ni}]^T$  are the width and center vectors of the Gaussian membership, respectively; and the Gaussian membership  $\phi_i$  represents as

$$\phi_i(\boldsymbol{\sigma}_i, \|\mathbf{z} - \mathbf{c}_i\|) = \prod_{j=1}^n \exp \left[ -\frac{(z_j - c_{ji})^2}{\sigma_{ji}^2} \right]. \quad (3)$$

For ease of notation, (2) can be expressed in a vector form as

$$\Xi = \boldsymbol{\alpha}^T \boldsymbol{\theta}(\mathbf{z}, \boldsymbol{\sigma}, \mathbf{c}) \quad (4)$$

where  $\boldsymbol{\alpha} = [\alpha_1, \alpha_2, \dots, \alpha_m]^T$ ;  $\boldsymbol{\theta} = [\theta_1, \theta_2, \dots, \theta_m]^T = [\psi_1 \phi_1, \psi_2 \phi_2, \dots, \psi_m \phi_m]^T$ ;  $\boldsymbol{\sigma} = [\boldsymbol{\sigma}_1, \boldsymbol{\sigma}_2, \dots, \boldsymbol{\sigma}_m]^T$  and  $\mathbf{c} = [\mathbf{c}_1, \mathbf{c}_2, \dots, \mathbf{c}_m]^T$ . There is an ideal FWNN can uniformly approximate any nonlinear function  $\Omega$  such as (Ho *et al.*, 2001)

$$\Omega = \boldsymbol{\alpha}^{*T} \boldsymbol{\theta}^*(\mathbf{z}, \boldsymbol{\sigma}^*, \mathbf{c}^*) + \Delta \quad (5)$$

where  $\boldsymbol{\alpha}^*$  and  $\boldsymbol{\theta}^*$  are the optimal parameter vectors of  $\boldsymbol{\alpha}$  and  $\boldsymbol{\theta}$ , respectively;  $\boldsymbol{\sigma}^*$  and  $\mathbf{c}^*$  are the optimal parameter vectors of  $\boldsymbol{\sigma}$  and  $\mathbf{c}$ , respectively; and  $\Delta$  is the approximation error. However, the optimal parameter vectors are unknown, so it is necessary to estimate the values by an estimated FWNN as following

$$\hat{\Xi} = \hat{\boldsymbol{\alpha}}^T \hat{\boldsymbol{\theta}}(\mathbf{z}, \hat{\boldsymbol{\sigma}}, \hat{\mathbf{c}}) \quad (6)$$

where  $\hat{\boldsymbol{\alpha}}$  and  $\hat{\boldsymbol{\theta}}$  are the estimated parameter vectors of  $\boldsymbol{\alpha}$  and  $\boldsymbol{\theta}$ , respectively; and  $\hat{\boldsymbol{\sigma}}$  and  $\hat{\mathbf{c}}$  are the estimated parameter vectors of  $\boldsymbol{\sigma}$  and  $\mathbf{c}$ , respectively. Then, the estimation error is obtained as

$$\begin{aligned} \tilde{\Xi} &= \Omega - \hat{\Xi} = \boldsymbol{\alpha}^{*T} \boldsymbol{\theta}^* - \hat{\boldsymbol{\alpha}}^T \hat{\boldsymbol{\theta}} + \Delta \\ &= (\tilde{\boldsymbol{\alpha}} + \hat{\boldsymbol{\alpha}})^T (\tilde{\boldsymbol{\theta}} + \hat{\boldsymbol{\theta}}) - \hat{\boldsymbol{\alpha}}^T \hat{\boldsymbol{\theta}} + \Delta \\ &= \tilde{\boldsymbol{\alpha}}^T \tilde{\boldsymbol{\theta}} + \tilde{\boldsymbol{\alpha}}^T \hat{\boldsymbol{\theta}} + \hat{\boldsymbol{\alpha}}^T \tilde{\boldsymbol{\theta}} + \Delta \end{aligned} \quad (7)$$

where  $\tilde{\boldsymbol{\alpha}} = \boldsymbol{\alpha}^* - \hat{\boldsymbol{\alpha}}$  and  $\tilde{\boldsymbol{\theta}} = \boldsymbol{\theta}^* - \hat{\boldsymbol{\theta}}$ . To speed up the convergence of the FWNN learning, the optimal parameter vector  $\boldsymbol{\alpha}^*$  and the estimated parameter vector  $\hat{\boldsymbol{\alpha}}$  decompose into three parts as (Golea *et al.*, 2002)

$$\boldsymbol{\alpha}^* = \eta_p \boldsymbol{\alpha}_p^* + \eta_l \boldsymbol{\alpha}_l^* + \eta_D \boldsymbol{\alpha}_D^* \quad (8)$$

$$\hat{\boldsymbol{\alpha}} = \eta_p \hat{\boldsymbol{\alpha}}_p + \eta_l \hat{\boldsymbol{\alpha}}_l + \eta_D \hat{\boldsymbol{\alpha}}_D \quad (9)$$

where  $\alpha_p^*$ ,  $\alpha_i^*$  and  $\alpha_d^*$  are the proportional, integral and derivative terms of  $\alpha^*$ , respectively;  $\hat{\alpha}_p$ ,  $\hat{\alpha}_i$  and  $\hat{\alpha}_d$  are the proportional, integral and derivative terms of  $\hat{\alpha}$ , respectively; and  $\eta_p$ ,  $\eta_i$  and  $\eta_d$  are positive coefficients specified by designers. Thus,  $\tilde{\alpha}$  can be expressed as

$$\tilde{\alpha} = \eta_i \tilde{\alpha}_i - \eta_p \hat{\alpha}_p - \eta_d \hat{\alpha}_d + \delta \quad (10)$$

where  $\tilde{\alpha}_i = \alpha_i^* - \hat{\alpha}_i$  and  $\delta = \eta_p \alpha_p^* + \eta_d \alpha_d^*$ . Substituting (10) into (7), it is obtained that

$$\begin{aligned} \tilde{\Xi} &= \tilde{\alpha}^T \tilde{\theta} + (\eta_i \tilde{\alpha}_i - \eta_p \hat{\alpha}_p - \eta_d \hat{\alpha}_d + \delta)^T \hat{\theta} + \hat{\alpha}^T \tilde{\theta} + \Delta \\ &= \eta_i \tilde{\alpha}_i^T \hat{\theta} - \eta_p \hat{\alpha}_p^T \hat{\theta} - \eta_d \hat{\alpha}_d^T \hat{\theta} + \hat{\alpha}^T \tilde{\theta} + \tilde{\alpha}^T \hat{\theta} + \delta^T \hat{\theta} + \Delta \end{aligned} \quad (11)$$

The Taylor expansion linearization technique is employed to transform the nonlinear function into a partially linear form, so (Lin, 2009)

$$\tilde{\theta} = \mathbf{A}^T \tilde{\sigma} + \mathbf{B}^T \tilde{c} + \mathbf{h} \quad (12)$$

where  $\tilde{\sigma} = \sigma^* - \hat{\sigma}$ ;  $\tilde{c} = c^* - \hat{c}$ ;  $\mathbf{h}$  is a vector of high order

terms;  $\mathbf{A} = \left[ \begin{array}{ccc} \frac{\partial \theta_1}{\partial \sigma} & \frac{\partial \theta_2}{\partial \sigma} & \dots & \frac{\partial \theta_m}{\partial \sigma} \end{array} \right]_{\sigma=\hat{\sigma}}$  and

$\mathbf{B} = \left[ \begin{array}{ccc} \frac{\partial \theta_1}{\partial c} & \frac{\partial \theta_2}{\partial c} & \dots & \frac{\partial \theta_m}{\partial c} \end{array} \right]_{c=\hat{c}}$ . Substitute (12) into (11),

yields

$$\begin{aligned} \tilde{\Xi} &= \eta_i \tilde{\alpha}_i^T \hat{\theta} - \eta_p \hat{\alpha}_p^T \hat{\theta} - \eta_d \hat{\alpha}_d^T \hat{\theta} + \hat{\alpha}^T (\mathbf{A}^T \tilde{\sigma} + \mathbf{B}^T \tilde{c} + \mathbf{h}) + \tilde{\alpha}^T \tilde{\theta} + \delta^T \hat{\theta} + \Delta \\ &= \eta_i \tilde{\alpha}_i^T \hat{\theta} - \eta_p \hat{\alpha}_p^T \hat{\theta} - \eta_d \hat{\alpha}_d^T \hat{\theta} + \tilde{\sigma}^T \mathbf{A} \hat{\alpha} + \tilde{c}^T \mathbf{B} \hat{\alpha} + \varepsilon \end{aligned} \quad (13)$$

where  $\hat{\alpha}^T \mathbf{A}^T \tilde{\sigma} = \tilde{\sigma}^T \mathbf{A} \hat{\alpha}$  and  $\hat{\alpha}^T \mathbf{B}^T \tilde{c} = \tilde{c}^T \mathbf{B} \hat{\alpha}$  are used since they are scalars; and  $\varepsilon = \hat{\alpha}^T \mathbf{h} + \tilde{\alpha}^T \tilde{\theta} + \delta^T \hat{\theta} + \Delta$  denotes the approximation error which is assumed to be bounded by  $0 \leq |\varepsilon| \leq E$  in which  $E$  is a positive constant.

### 3. DESIGN OF THE AFWNNC SYSTEM

Consider a class of  $n$ -th order nonlinear systems

$$\dot{x}^{(n)} = f(\mathbf{x}) + gu \quad (14)$$

where  $\mathbf{x} = [x, \dot{x}, \dots, x^{(n-1)}]^T$  is the state vector of the system which is assumed to be available for measurement;  $f(\mathbf{x})$  is a real continuous function;  $g$  is the control gain of the system; and  $u$  is the control input. The control objective is to find a control law so the state trajectory  $x$  can track a trajectory command  $x_c$ . To determine the control law, a tracking error is defined as

$$e = x_c - x. \quad (15)$$

If the system parameters in (14) are known, there exists an ideal controller as (Slotine and Li, 1991)

$$u^* = g^{-1}[-f(\mathbf{x}) + x_c^{(n)} + k_1 e^{(n-1)} + \dots + k_{n-1} \dot{e} + k_n e] \quad (16)$$

where  $k_i$ ,  $i = 1, 2, \dots, n$  are nonzero positive constant. Apply this ideal controller (16) into system dynamic (14), it can be obtained

$$e^{(n)} + k_1 e^{(n-1)} + \dots + k_{n-1} \dot{e} + k_n e = 0. \quad (17)$$

If the parameter  $k_i$  is selected to satisfy that all roots will lie on left half side of  $s$ -plane, it implies  $\lim_{t \rightarrow \infty} e = 0$ . However, because the system dynamics in (14) are actually unknown, the ideal controller (16) cannot be utilized.

In this paper, the AFWNNC system shown in Fig. 1 is designed to resolve this problem which the controller output is designed as

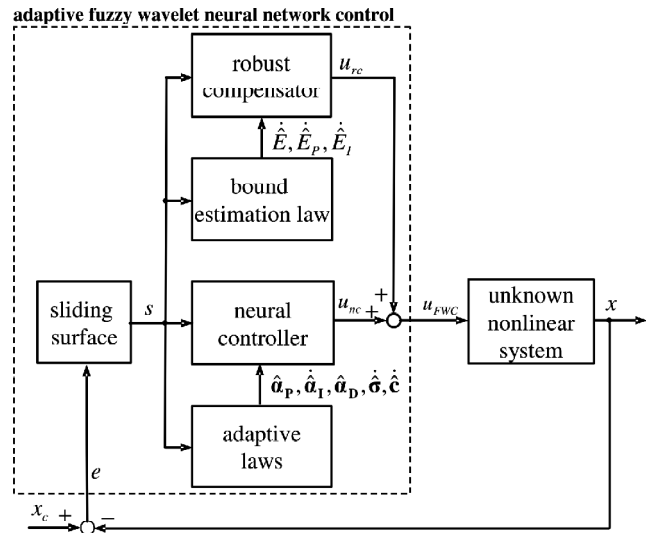


Figure 1: The Block Diagram of the AFWNNC System

$$u_{FWC} = u_{nc} + u_{rc} \quad (18)$$

where a sliding surface is defined as

$$s = e^{(n-1)} + k_1 e^{(n-2)} + \dots + k_{n-1} e + k_n \int_0^t e(\tau) d\tau \quad (19)$$

The neural controller  $u_{nc}$  utilizes a FWN to mimic the ideal controller, and the robust compensator  $u_{rc}$  is designed to compensate for the difference between the ideal controller and neural controller. In the sliding-mode control approach, the sliding condition is derived as  $s \dot{s} < 0$  such that the stability and convergence of  $s \rightarrow 0$  as  $t \rightarrow \infty$  can be guaranteed for the closed-loop system (Slotine and Li, 1991). Substituting (18) into (14) and using (16) and (19), yields

$$e^{(n)} + k_1 e^{(n-1)} + \dots + k_{n-1} \dot{e} + k_n e = g(u^* - u_{nc} - u_{rc}) = \dot{s} \quad (20)$$

By using the approximation property (13), (20) can be rewritten as

$$\dot{s} = g(\eta_i \tilde{\alpha}_i^T \hat{\theta} - \eta_p \hat{\alpha}_p^T \hat{\theta} - \eta_d \hat{\alpha}_d^T \hat{\theta} + \tilde{\sigma}^T \mathbf{A} \hat{\alpha} + \tilde{c}^T \mathbf{B} \hat{\alpha} + \varepsilon - u_{rc}) \quad (21)$$

In this paper, the robust compensator is designed as

$$u_{rc} = \begin{cases} \hat{E} \operatorname{sgn}(s) & \text{for } |s| > \Phi \\ \hat{E}_p s + \hat{E}_I \int s dt = \hat{\zeta}^T \xi & \text{for } |s| \leq \Phi \end{cases} \quad (22)$$

where  $\hat{E}$ ,  $\hat{E}_p$  and  $\hat{E}_I$  are free controller parameters;  $\Phi > 0$  is the thickness of the boundary layer;  $\hat{\zeta} = [\hat{E}_p, \hat{E}_I]^T$ ; and  $\xi = [s, \int s dt]^T$ . When the sliding surface is within the boundary layer ( $|s| \leq \Phi$ ), the robust compensator is defined as  $u_{rc} = \hat{E}_p s + \hat{E}_I \int s dt$ ; and when the sliding surface is outside the boundary layer ( $|s| > \Phi$ ), the robust compensator is defined as  $u_{rc} = \hat{E} \operatorname{sgn}(s)$ . The parameters  $\hat{E}$ ,  $\hat{E}_p$  and  $\hat{E}_I$  are not known in advance. To guarantee the stability of the proposed AFWNNC system, two cases are considered separately depending on the value of  $|s|$ .

Case 1: For  $|s| > \Phi$ , a Lyapunov function is defined as

$$V_1 = \frac{s^2}{2} + g \left( \frac{\eta_I}{2} \tilde{\mathbf{a}}_1^T \tilde{\mathbf{a}}_1 + \frac{\eta_D}{2} \hat{\mathbf{a}}_p^T \hat{\mathbf{a}}_p + \frac{\tilde{\boldsymbol{\sigma}}^T \tilde{\boldsymbol{\sigma}}}{2\eta_\sigma} + \frac{\tilde{\mathbf{c}}^T \tilde{\mathbf{c}}}{2\eta_c} + \frac{\tilde{E}^2}{2\eta_E} \right) \quad (23)$$

where  $\tilde{E} = E - \hat{E}$ . Differentiating (23) with respect to time and using (21), it is obtained that

$$\begin{aligned} \dot{V}_1 &= s\dot{s} + g\eta_I \tilde{\mathbf{a}}_1^T \dot{\tilde{\mathbf{a}}}_1 + g\eta_D \hat{\mathbf{a}}_p^T \dot{\hat{\mathbf{a}}}_p + \frac{g}{\eta_\sigma} \tilde{\boldsymbol{\sigma}}^T \dot{\tilde{\boldsymbol{\sigma}}} + \frac{g}{\eta_c} \tilde{\mathbf{c}}^T \dot{\tilde{\mathbf{c}}} + \frac{g}{\eta_E} \tilde{E} \dot{\tilde{E}} \\ &= g\eta_I \tilde{\mathbf{a}}_1^T (s\hat{\boldsymbol{\theta}} + \dot{\hat{\mathbf{a}}}_1) + g\tilde{\boldsymbol{\sigma}}^T \left[ s\mathbf{A}\hat{\mathbf{a}} + \frac{\dot{\tilde{\boldsymbol{\sigma}}}}{\eta_\sigma} \right] + g\tilde{\mathbf{c}}^T \left[ s\mathbf{B}\hat{\mathbf{a}} + \frac{\dot{\tilde{\mathbf{c}}}}{\eta_c} \right] \\ &\quad + sg(-\eta_p \hat{\mathbf{a}}_p^T \hat{\boldsymbol{\theta}} - \eta_D \hat{\mathbf{a}}_p^T \dot{\hat{\boldsymbol{\theta}}} + \varepsilon - u_{rc}) + g\eta_D \hat{\mathbf{a}}_p^T \dot{\hat{\mathbf{a}}}_p + \frac{g}{\eta_E} \tilde{E} \dot{\tilde{E}} \end{aligned} \quad (24)$$

Choose the adaptive laws as

$$\dot{\tilde{\mathbf{a}}}_1 = -\dot{\hat{\mathbf{a}}}_1 = -s\hat{\boldsymbol{\theta}} \quad (25)$$

$$\dot{\tilde{\boldsymbol{\sigma}}} = -\dot{\tilde{\boldsymbol{\sigma}}} = -\eta_\sigma s \mathbf{A} \hat{\mathbf{a}} \quad (26)$$

$$\dot{\tilde{\mathbf{c}}} = -\dot{\tilde{\mathbf{c}}} = -\eta_c s \mathbf{B} \hat{\mathbf{a}} \quad (27)$$

then (24) can be obtained

$$\dot{V}_1 = sg(\varepsilon - u_{rc}) - g\eta_p \hat{\mathbf{a}}_p^T s\hat{\boldsymbol{\theta}} - g\eta_D \hat{\mathbf{a}}_p^T s\dot{\hat{\boldsymbol{\theta}}} + g\eta_D \hat{\mathbf{a}}_p^T \dot{\hat{\mathbf{a}}}_p + \frac{g}{\eta_E} \tilde{E} \dot{\tilde{E}} \quad (28)$$

Since  $\hat{\mathbf{a}}_p$ ,  $\hat{\mathbf{a}}_1$  and  $\hat{\mathbf{a}}_D$  are the proportional, integral and derivative terms of  $\hat{\mathbf{a}}$ , respectively; the controller parameter vectors are chosen as

$$\hat{\mathbf{a}}_p = s\hat{\boldsymbol{\theta}} \quad (29)$$

$$\hat{\mathbf{a}}_D = \dot{\hat{\mathbf{a}}}_p \quad (30)$$

and the approximation error bound estimation law is designed as

$$\dot{\tilde{E}} = -\dot{\tilde{E}} = -\eta_E |s| \quad (31)$$

then (28) can be obtained

$$\begin{aligned} \dot{V}_1 &= g\varepsilon s - g\tilde{E}|s| - g\eta_p \hat{\mathbf{a}}_p^T \hat{\mathbf{a}}_p - g(E - \hat{E})|s| \\ &= g\varepsilon s - gE|s| - g\eta_p \hat{\mathbf{a}}_p^T \hat{\mathbf{a}}_p \\ &\leq g|\varepsilon||s| - gE|s| \\ &= -g|s|(E - |\varepsilon|) \leq 0. \end{aligned} \quad (32)$$

Since  $\dot{V}_1(s, \tilde{\mathbf{a}}_1, \hat{\mathbf{a}}_p, \tilde{\boldsymbol{\sigma}}, \tilde{\mathbf{c}}, \tilde{E}, t)$  is negative semi-definite, that is  $V_1(s, \tilde{\mathbf{a}}_1, \hat{\mathbf{a}}_p, \tilde{\boldsymbol{\sigma}}, \tilde{\mathbf{c}}, \tilde{E}, t) \leq V_1(s, \tilde{\mathbf{a}}_1, \hat{\mathbf{a}}_p, \tilde{\boldsymbol{\sigma}}, \tilde{\mathbf{c}}, \tilde{E}, 0)$ , it implies that  $s$ ,  $\tilde{\mathbf{a}}_1$ ,  $\hat{\mathbf{a}}_p$ ,  $\tilde{\boldsymbol{\sigma}}$ ,  $\tilde{\mathbf{c}}$  and  $\tilde{E}$  are bounded. Define the following term

$$\Theta(t) \equiv gs(E - |\varepsilon|) \leq -\dot{V}_1 \quad (33)$$

and integrate  $\Theta(t)$  with respect to time, then it is obtained that

$$\int_0^t \Theta(\tau) d\tau \leq V_1(s, \tilde{\mathbf{a}}_1, \hat{\mathbf{a}}_p, \tilde{\boldsymbol{\sigma}}, \tilde{\mathbf{c}}, \tilde{E}, 0) - V_1(s, \tilde{\mathbf{a}}_1, \hat{\mathbf{a}}_p, \tilde{\boldsymbol{\sigma}}, \tilde{\mathbf{c}}, \tilde{E}, t) \quad (34)$$

Because  $V_1(s, \tilde{\mathbf{a}}_1, \hat{\mathbf{a}}_p, \tilde{\boldsymbol{\sigma}}, \tilde{\mathbf{c}}, \tilde{E}, 0)$  is bounded and  $V_1(s, \tilde{\mathbf{a}}_1, \hat{\mathbf{a}}_p, \tilde{\boldsymbol{\sigma}}, \tilde{\mathbf{c}}, \tilde{E}, t)$  is nonincreasing and bounded, the following result can be obtained

$$\lim_{t \rightarrow \infty} \int_0^t \Theta(\tau) d\tau < \infty. \quad (35)$$

By Barbalat's Lemma, it shows  $\lim_{t \rightarrow \infty} \Theta = 0$ . That is  $s \rightarrow 0$  as  $t \rightarrow \infty$  (Slotine and Li, 1991). As a result, the AFWNNC system is asymptotically stable when the sliding surface is outside the boundary layer ( $|s| > \Phi$ ).

Case 2: For  $|s| \leq \Phi$ , a Lyapunov function is defined as

$$V_2 = \frac{s^2}{2} + g \left[ \frac{\eta_I}{2} \tilde{\mathbf{a}}_1^T \tilde{\mathbf{a}}_1 + \frac{\eta_D}{2} \hat{\mathbf{a}}_p^T \hat{\mathbf{a}}_p + \frac{\tilde{\boldsymbol{\sigma}}^T \tilde{\boldsymbol{\sigma}}}{2\eta_\sigma} + \frac{\tilde{\mathbf{c}}^T \tilde{\mathbf{c}}}{2\eta_c} + \frac{\tilde{\zeta}^T \tilde{\zeta}}{2\eta_\zeta} \right] \quad (36)$$

where the positive constant  $\eta_\zeta$  is the learning rate;  $\tilde{\zeta} = \boldsymbol{\zeta}^* - \hat{\boldsymbol{\zeta}}$  and  $\boldsymbol{\zeta}^*$  is the optimal value for  $\boldsymbol{\zeta}$  as defined

$$\boldsymbol{\zeta}^* = \arg \min_{\boldsymbol{\zeta} \in \mathbb{R}^2} \left[ \sup_{s \in \mathbb{R}} |\hat{\boldsymbol{\zeta}}^T \boldsymbol{\zeta} - E \operatorname{sgn}(s)| \right]. \quad (37)$$

Taking the derivative of Lyapunov function (36) and using (25)-(30), yields

$$\begin{aligned}
\dot{V}_2 &= s\dot{s} + g\eta_l \tilde{\mathbf{a}}_1^T \dot{\tilde{\mathbf{a}}}_1 + g\eta_D \hat{\mathbf{a}}_p^T \dot{\tilde{\mathbf{a}}}_p + \frac{g}{\eta_\sigma} \tilde{\boldsymbol{\sigma}}^T \dot{\tilde{\boldsymbol{\sigma}}} + \frac{g}{\eta_c} \tilde{\mathbf{c}}^T \dot{\tilde{\mathbf{c}}} + \frac{g}{\eta_\zeta} \tilde{\boldsymbol{\zeta}}^T \dot{\tilde{\boldsymbol{\zeta}}} \\
&= g\eta_l \tilde{\mathbf{a}}_1^T (s\dot{\boldsymbol{\theta}} + \dot{\tilde{\mathbf{a}}}_1) + g\tilde{\boldsymbol{\sigma}}^T \left[ s\mathbf{A}\hat{\mathbf{a}} + \frac{\dot{\tilde{\boldsymbol{\sigma}}}}{\eta_\sigma} \right] + g\tilde{\mathbf{c}}^T \left[ s\mathbf{B}\hat{\mathbf{a}} + \frac{\dot{\tilde{\mathbf{c}}}}{\eta_c} \right] \\
&\quad + sg(-\eta_p \hat{\mathbf{a}}_p^T \dot{\boldsymbol{\theta}} - \eta_D \hat{\mathbf{a}}_D^T \dot{\boldsymbol{\theta}} + \varepsilon - u_{rc}) + g\eta_D \hat{\mathbf{a}}_p^T \dot{\tilde{\mathbf{a}}}_p + \frac{g}{\eta_\zeta} \tilde{\boldsymbol{\zeta}}^T \dot{\tilde{\boldsymbol{\zeta}}} \\
&= sg(\varepsilon - u_{rc}) - g\eta_p \hat{\mathbf{a}}_p^T \dot{\tilde{\mathbf{a}}}_p + \frac{g}{\eta_\zeta} \tilde{\boldsymbol{\zeta}}^T \dot{\tilde{\boldsymbol{\zeta}}} \\
&\leq sg(\varepsilon - \hat{\boldsymbol{\zeta}}^T \boldsymbol{\xi}) + \frac{g}{\eta_c} \tilde{\boldsymbol{\zeta}}^T \dot{\tilde{\boldsymbol{\zeta}}} \\
&= sg(\varepsilon - \hat{\boldsymbol{\zeta}}^T \boldsymbol{\xi} + \boldsymbol{\zeta}^{*T} \boldsymbol{\xi} - \boldsymbol{\zeta}^{*T} \boldsymbol{\xi}) + \frac{g}{\eta_c} \tilde{\boldsymbol{\zeta}}^T \dot{\tilde{\boldsymbol{\zeta}}} \\
&= sg(\varepsilon - \tilde{\boldsymbol{\zeta}}^T \boldsymbol{\xi} - \boldsymbol{\zeta}^{*T} \boldsymbol{\xi}) + \frac{g}{\eta_c} \tilde{\boldsymbol{\zeta}}^T \dot{\tilde{\boldsymbol{\zeta}}} \\
&= g\tilde{\boldsymbol{\zeta}}^T \left[ s\boldsymbol{\xi} + \frac{1}{\eta_c} \dot{\tilde{\boldsymbol{\zeta}}} \right] + sg\varepsilon - sg\boldsymbol{\zeta}^{*T} \boldsymbol{\xi} \quad (38)
\end{aligned}$$

It can find  $\hat{\boldsymbol{\zeta}}^T \boldsymbol{\xi}$  lies in the first and third quadrant and  $s\hat{\boldsymbol{\zeta}}^T \boldsymbol{\xi} = 0$  for  $s = 0$ . It concludes  $s\boldsymbol{\zeta}^{*T} \boldsymbol{\xi} = |s| |\boldsymbol{\zeta}^{*T} \boldsymbol{\xi}|$ . If the adaptation laws is chosen as

$$\dot{\tilde{\boldsymbol{\zeta}}} = -\dot{\hat{\boldsymbol{\zeta}}} = -\eta_\zeta s \boldsymbol{\xi} \quad (39)$$

then (38) can be rewritten as

$$\begin{aligned}
\dot{V}_2 &\leq |E| |s| |g - sg\hat{\boldsymbol{\zeta}}^T \boldsymbol{\xi}| \\
&\leq E |s| |g - |s| |\boldsymbol{\zeta}^{*T} \boldsymbol{\xi}| |g| \\
&= -(|\boldsymbol{\zeta}^{*T} \boldsymbol{\xi}| - E) |s| |g| \leq 0. \quad (40)
\end{aligned}$$

Similar to the proof of (32), it can be similarly shown that  $s \rightarrow 0$  as  $t \rightarrow \infty$ . As a result, the AFWNNC system is asymptotically stable when the sliding surface is within the boundary layer ( $|s| \leq \Phi$ ).

#### 4. SIMULATION AND EXPERIMENTAL RESULTS

In this section, the proposed AFWNNC system is applied to a chaotic system and a DC motor to verify its effectiveness. It should be emphasized the development of the AFWNNC system doesn't need to know the knowledge of the system dynamics. For practical implementation, the parameters of the AFWNNC system can be online tuned by the proposed adaptive laws.

*Example 1:* chaotic system

Chaotic system is a nonlinear deterministic system that displays complex, noisy-like and unpredictable behavior

(Peng and Hsu, 2009). It can be observed in many nonlinear circuits and mechanical systems. For control engineers, control of a chaotic system has become a significant research topic in physics, mathematics and engineering communities. Consider a second-order chaotic system such as the Duffing's equation describing a special nonlinear circuit or a pendulum moving in a viscous medium (Peng and Hsu, 2009)

$$\ddot{x} = f(\mathbf{x}) + u \quad (41)$$

where  $f(\mathbf{x}) = -p\dot{x} - p_1x - p_2x^3 + q \cos(\omega t)$  is the system dynamics,  $t$  is the time variable,  $\omega$  is the frequency,  $u$  is the control effort and  $p, p_1, p_2$  and  $q$  are real constants. For observing the chaotic unpredictable behavior, the open-loop system behavior with  $u = 0$  was simulated with  $p = 0.4, p_1 = -1.1, p_2 = 1.0$  and  $\omega = 1.8$ . The phase plane plots from an initial condition point  $(0, 0)$  are shown in Figs. 2(a) and 2(b) for  $q = 2.1$  and  $q = 7.0$ , respectively. It is shown the uncontrolled chaotic system has different chaotic trajectories with different  $q$  values.

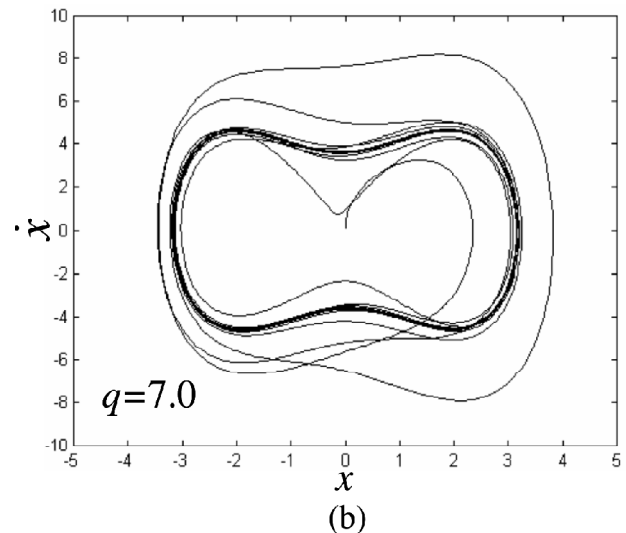
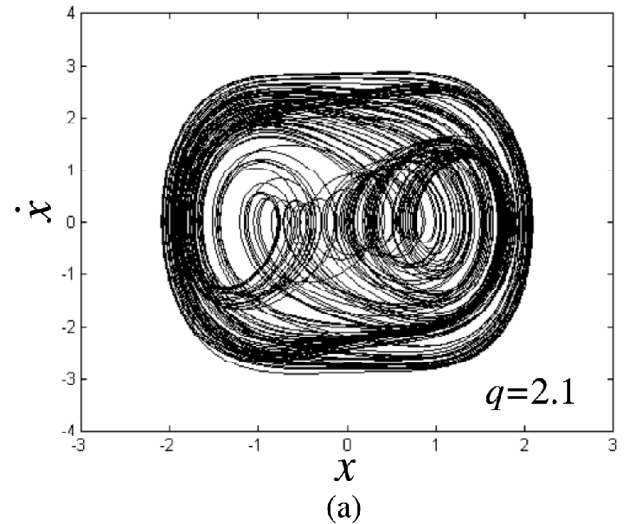


**Figure 2:** Phase Plane of Uncontrolled Chaotic System

The proposed AFWNNC system is applied to the chaotic system. There are 5 rules in the used FWNN with the sliding surface  $s$  as the input variable. The parameters  $\omega_{ki}$  in the “Mexican hat” mother wavelet function are fixed as  $\omega_{ki} = 2$  for  $k = 1$  and  $i = 1, 2, \dots, 5$ ; the parameter vectors of the Gaussian membership functions are initialized from  $\sigma = [0.3, 0.3, 0.3, 0.3, 0.3]^T$  and  $\mathbf{c} = [-1.0, -0.5, 0.0, 0.5, 1.0]^T$ ; and the initial output connections  $\alpha_i$  are initiated from zeros. The choices of these initial values are through some trials to achieve satisfactory control performance. There are 15 parameters can be online tuned by the derived adaptive laws in the used FWNN. The control parameters of the AFWNNC system are selected as  $k_1 = 2$ ,  $k_2 = 1$ ,  $\eta_I = 10$ ,  $\eta_p = 1$ ,  $\eta_D = 0.1$ ,  $\eta_\sigma = \eta_c = 1$ ,  $\Phi = 0.5$  and  $\eta_E = \eta_\zeta = 0.1$ . All the gains in the AFWNNC system are chosen to consider the requirement of stability condition. Properly choosing the values of  $k_1$  and  $k_2$ , the desired system dynamics such as rise time, overshoot, and settling time can be easily designed by the second-order system. The parameters  $\eta_p$ ,  $\eta_D$ ,  $\eta_\sigma$  and  $\eta_c$  are the leaning rates of the interconnection weights of FWNN; and the parameters  $\eta_E$  and  $\eta_\zeta$  are the leaning rates of the robust compensator. If the leaning rate parameters are chosen to be small, then the parameters convergence of the AFWNNC system will be easily achieved; however, this will result in slow learning speed.

A performance index  $I$  is defined as  $I = \sum(e^2 + \dot{e}^2)$ . As  $\eta_p = \eta_D = 0$ , the learning algorithm of the proposed method is the same as conventional AFWNNC system with integral type adaptation laws in the previous published papers (Lin, 2006; Zekri *et al.*, 2008; Lin, 2009). The simulation results of the AFWNNC system with integral type adaptation laws are shown in Figs. 3 and 4 for  $q = 2.1$  and  $q = 7.0$ , respectively. The tracking responses of state  $x$  are shown in Figs. 3(a) and 4(a); the tracking responses of state  $\dot{x}$  are shown in Figs. 3(b) and 4(b); the associated control efforts are shown in Figs. 3(c) and 4(c); the performance indexes are shown in Figs. 3(d) and 4(d); and the output connections  $\hat{\alpha}$  are shown Figs. 3(e) and 4(e) for  $q = 2.1$  and  $q = 7.0$ , respectively. The simulation results show there is no chattering phenomena in the control effort; however, the convergence of controller parameter and tracking error is slow. Then, the developed PID type adaptation law is applied to the AFWNNC system. The simulation results of the AFWNNC system with PID type adaptation laws are shown in Figs. 5 and 6 for  $q = 2.1$  and  $q = 7.0$ , respectively. The tracking responses of state  $x$  are shown in Figs. 5(a) and 6(a); the tracking responses of state  $\dot{x}$  are shown in Figs. 5(b) and 6(b); the associated control efforts are shown in Figs. 5(c) and 6(c); the performance indexes are shown in Figs. 5(d) and 6(d); and the output connections  $\hat{\alpha}$  are shown in Figs. 5(e) and 6(e) for  $q = 2.1$  and  $q = 7.0$ , respectively. The simulation results show the proposed PID type adaptation laws can achieve faster convergence of the

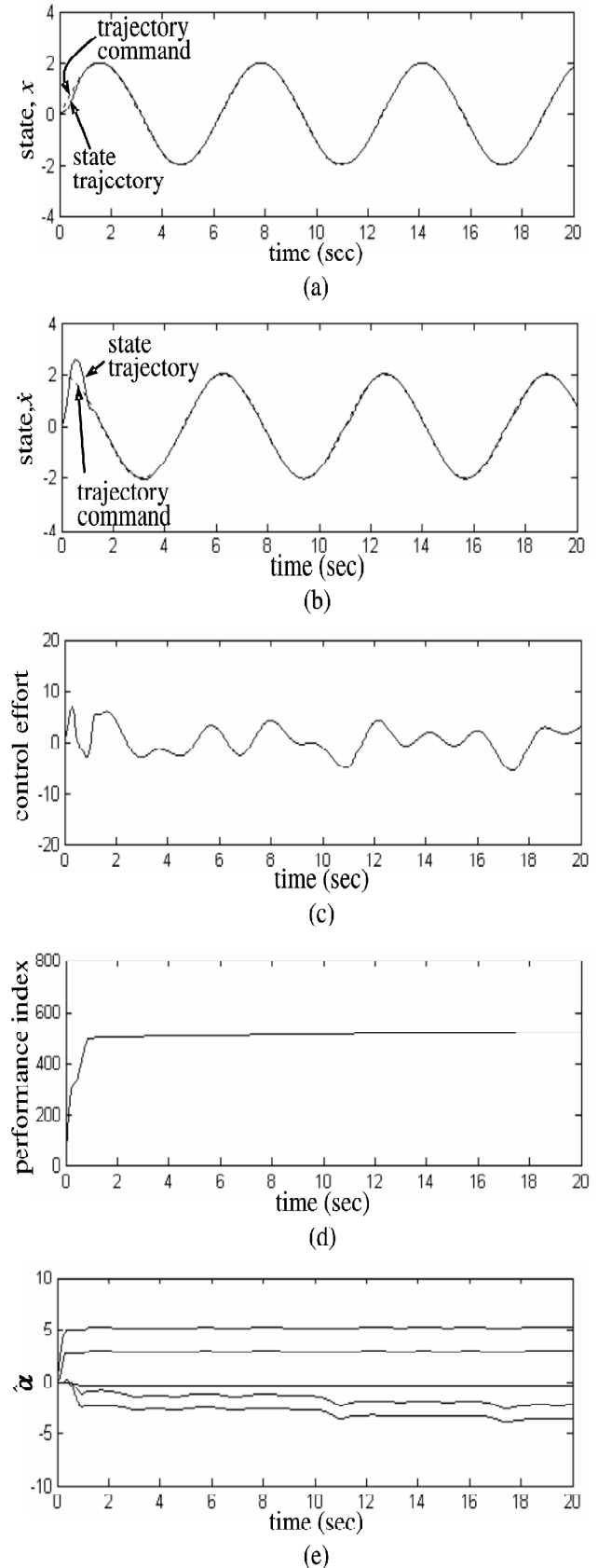


**Figure 3:** Simulation Results of AFWNNC with Integral Type Adaptation Laws for  $q = 2.1$

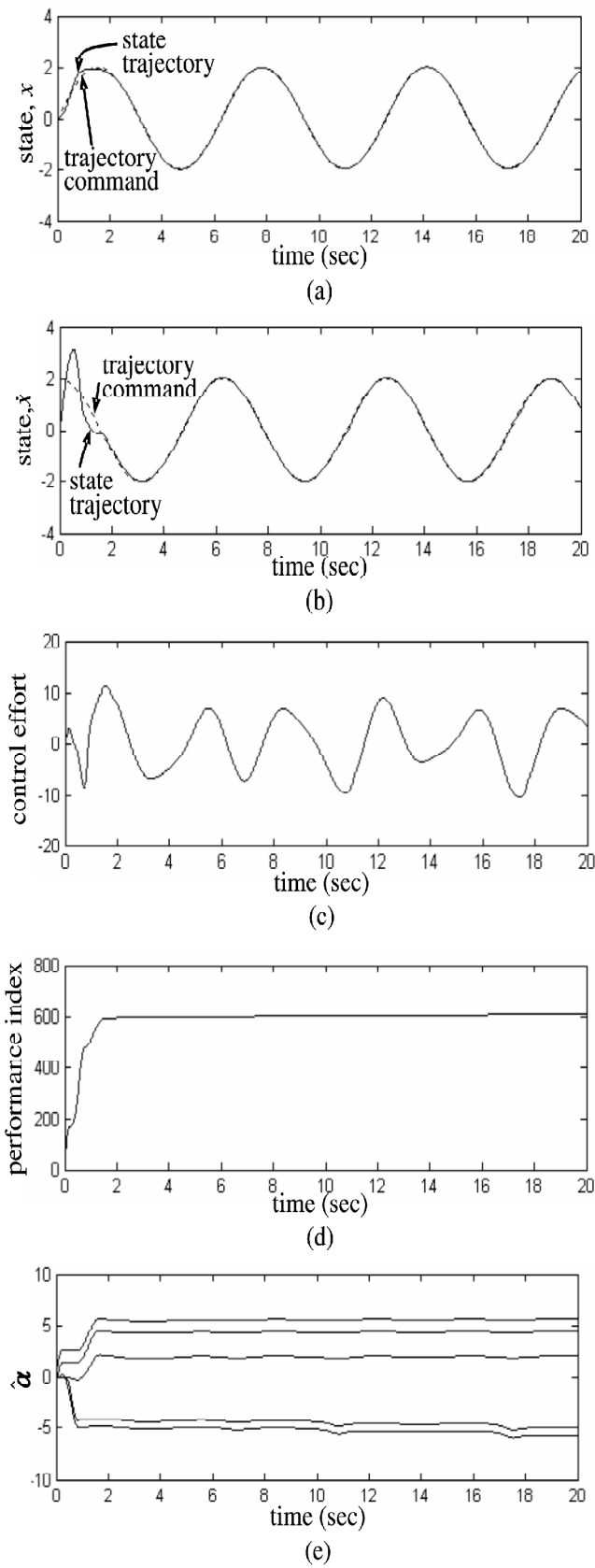


**Figure 4:** Simulation Results of AFWNNC with Integral Type Adaptation Laws for  $q = 7.0$

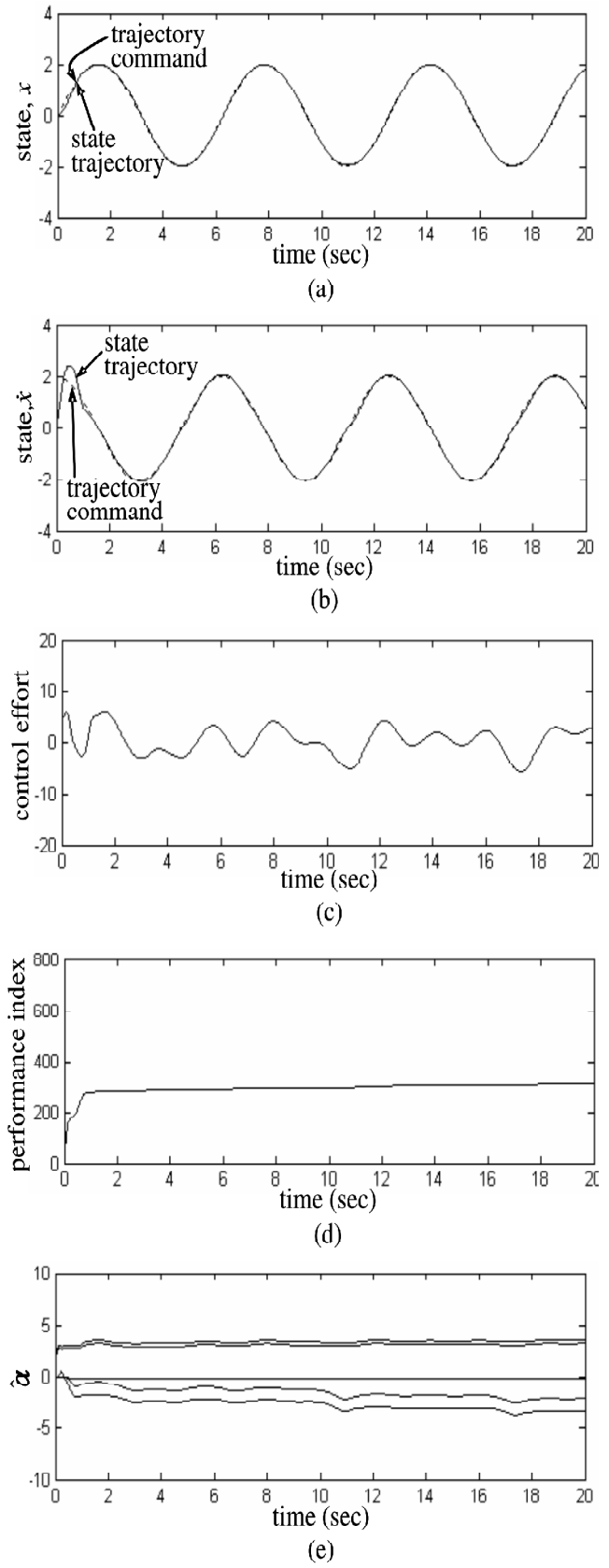


**Figure 5:** Simulation Results of AFWNNC with PID Type Adaptation Laws for  $q = 2.1$

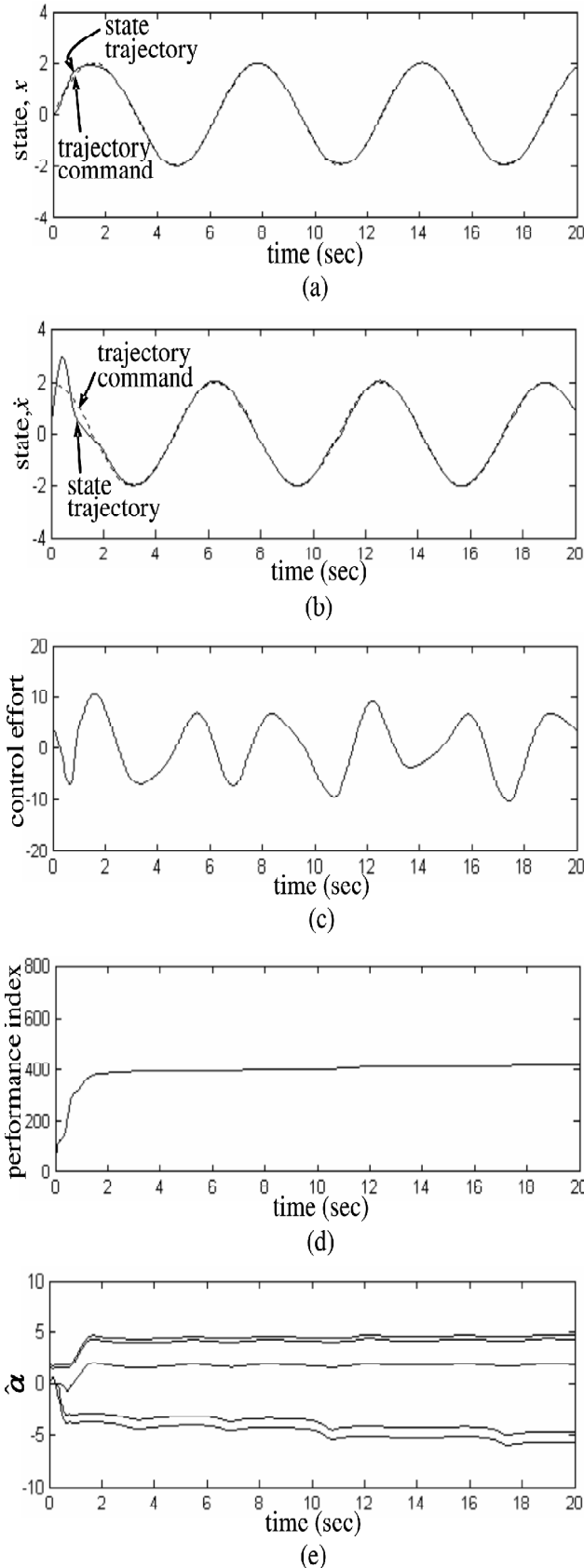


Figure 6: Simulation Results of AFWNNC with PID Type Adaptation Laws for  $q = 7.0$

tracking error and controller parameters than that using integral type adaptation laws.

Example 2: DC motor

The equation of a DC motor can be simplified as (Damiano *et al.*, 2004; Nouri *et al.*, 2008)

$$v_a = r_a i_a + l_a \frac{di_a}{dt} + k_b \dot{\theta} \tag{42}$$

$$J\ddot{\theta} + B\dot{\theta} = k_t i_a \tag{43}$$

where  $r_a, l_a, k_b$  and  $k_t$  are the DC motor parameters that are unknown;  $v_a$  and  $i_a$  are the DC motor voltage and current, respectively;  $\theta$  is the rotor position;  $J$  is the moment of inertia; and  $B$  is the damping coefficient. The standard canonical form of DC motor can be expressed as

$$\ddot{x} = f(x) + gu \tag{44}$$

where  $x = [\theta, \dot{\theta}, \ddot{\theta}]^T$ ;  $u = v_a$ ;

$f(x) = -\left(\frac{B}{J} + \frac{r_a}{l_a}\right)x_3 - \left(\frac{Br_a + k_t k_b}{Jl_a}\right)x_2$  and  $g = \frac{k_t}{Jl_a}$ . The

experimental setup as shown in Fig. 7 is based on a field programmable gate array (FPGA). FPGA is a fast prototyping IC component. It consists of thousands of logic gates, some of which are combined together to form a configurable logic block thereby simplifying high-level circuit design ([Online] <http://www.altera.com/>). The advantage of a controller implemented by FPGA includes shorter development cycles, lower cost, small size, fast system execute speed, and high flexibility. The proposed AFWNNC system is applied to the DC motor. There are 7 rules in the used FWNN with the sliding surface  $s$  as the input variable. The parameters  $\omega_{ki}$  in the ‘‘Mexican hat’’ mother wavelet function are fixed as  $\omega_{ki} = 1$  for  $k = 1$  and  $i = 1, 2, \dots, 7$ ; the parameter vectors of the Gaussian membership functions are initial from  $\sigma = [0.2, 0.2, 0.2,$

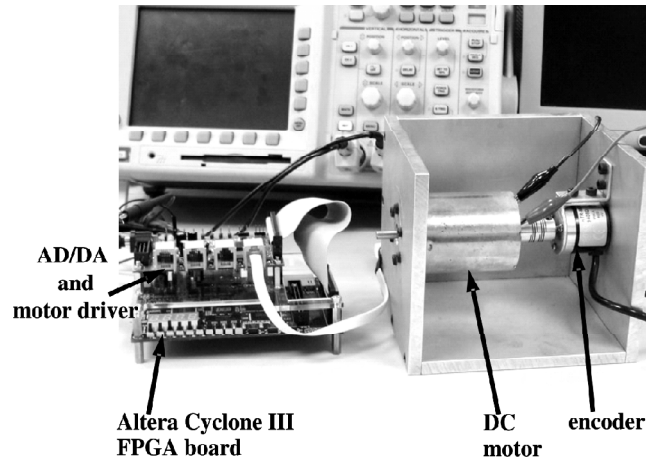


Figure 7: The Experimental Setup

$0.2, 0.2, 0.2, 0.2]^T$  and  $\mathbf{c} = [-1, -0.6, -0.3, 0, 0.3, 0.6, 1]^T$ ; and the initial output connections  $\alpha_i$  are initiated from zeros. The choices of these initial values are through some trials to achieve satisfactory control performance. Moreover, a second-order transfer function is chosen as the reference model for a periodic step command

$$\frac{w_n^2}{S^2 + 2\xi w_n S + w_n^2} = \frac{64}{S^2 + 16S + 64} \quad (45)$$

where  $S$  is the Laplace operator;  $\xi$  and  $w_n$  are the damping ratio and undamped natural frequency. To illustrate the effectiveness of the proposed design method, a comparison between a supervisory recurrent fuzzy neural network control (Lin & Hsu, 2004), the proposed AFWNNC system with integral type adaptation law and the proposed AFWNNC system with PID type adaptation law is made.

First, the supervisory recurrent fuzzy neural network control (Lin & Hsu, 2004) is applied to the DC motor. The experimental results of the supervisory recurrent fuzzy neural network control system are shown in Fig. 8. The tracking response is shown in Fig. 8(a); the associated control effort is shown in Fig. 8(b); and the tracing error is shown in

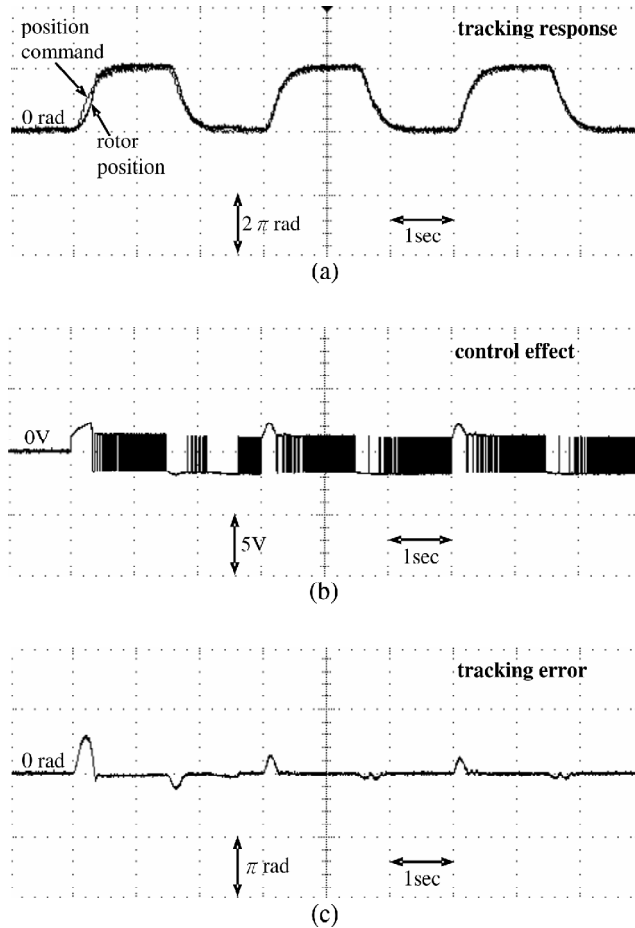


**Figure 8:** Experimental Results of Supervisory Recurrent Fuzzy Neural Network Control

Fig. 8(c). The experimental results show favorable tracking performance can be achieved; however, the convergence of the controller parameter and tracking error is slow. And, there exists the undesirable control chattering in Fig. 8(b). Then, the AFWNNC system is applied to the DC motor again. The control parameters are selected as  $k_1 = 6, k_2 = 12, k_3 = 8, \eta_c = \eta_e = 1, \Phi = 0.5$  and  $\eta_E = \eta_\xi = 0.1$ . All the gains in the AFWNNC system are chosen to achieve good transient control performance in the experiment considering the requirement of stability condition. The experimental results of the AFWNNC system with integral type adaptation law ( $\eta_i = 30, \eta_p = \eta_d = 0$ ) are shown in Fig. 9. The tracking response is shown in Fig. 9(a); the associated control effort is shown in Fig. 9(b); and the tracing error is shown in Fig. 9(c). The experimental results show favorable tracking performance can be achieved; however, the convergence of the controller parameter and tracking error is slow. The experimental results of the AFWNNC system with PID type adaptation law ( $\eta_i = 30, \eta_p = 5, \eta_d = 0.1$ ) are shown in Fig. 10. The tracking response is shown in Fig. 10(a); the associated control effort is shown in Fig. 10(b); and the tracing error is shown in Fig. 10(c). The experimental results show the favorable tracking performance and no chattering

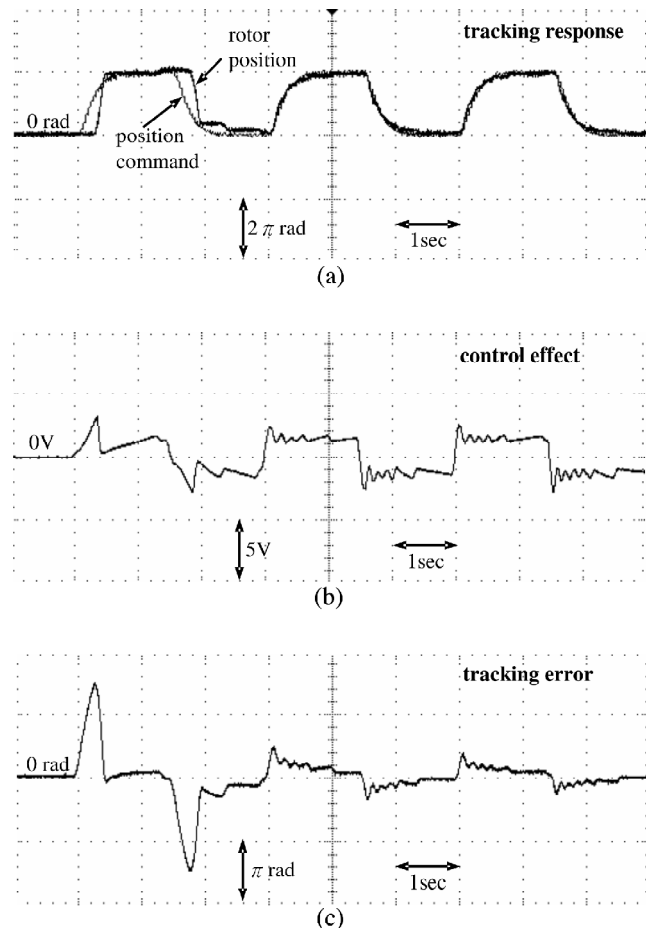


**Figure 9:** Experimental Results of AFWNNC with Integral Type Adaptation Laws

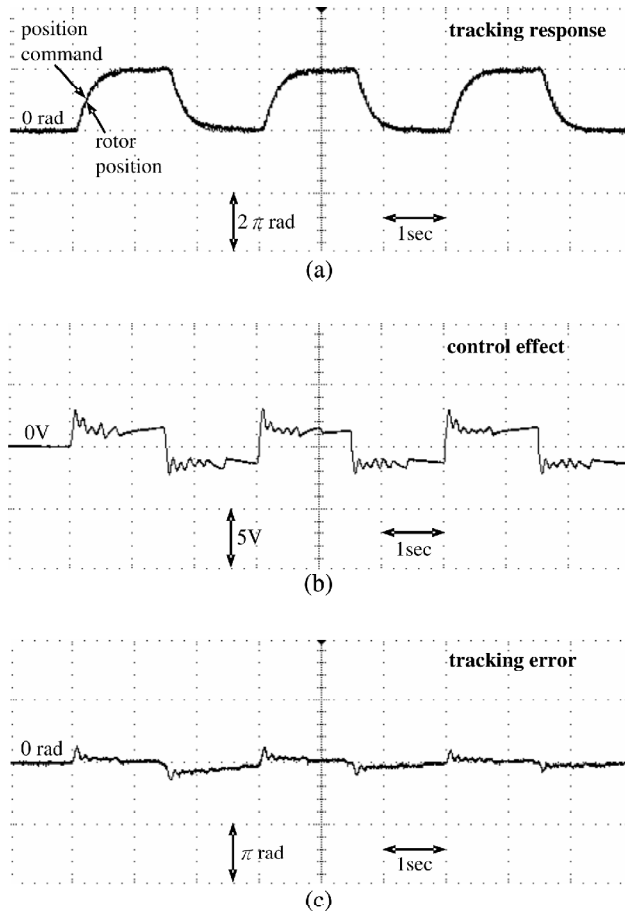


**Figure 10:** Experimental Results of AFWNNC with PID Type Adaptation Laws

phenomena can be achieved and the convergence of controller parameter and tracking error converge quickly with pay the price of a little larger computational load. In summary, a comparison of the control performance and

control characteristics between the supervisory recurrent fuzzy neural network control, the AFWNNC system with integral type adaptation law and the AFWNNC system with PID type adaptation law is summarized in Table 1. It is seen the PID type adaptation law can achieve better tracking performance than integral type adaptation law. Moreover, the robust compensator not only can guarantee system stability but also does not result in any chattering phenomena.

## 5. CONCLUSIONS

This paper has successfully implemented an adaptive fuzzy wavelet neural network control (AFWNNC) system for a chaotic system and a DC motor. The proposed AFWNNC system is composed of a neural controller with PID learning law and a robust compensator. The PID learning law can speed up the convergence of controller parameter and tracking error, and the robust compensator can dispel the approximation error to guarantee system stable based on the Lyapunov stability theorem. Finally, the effectiveness of the proposed AFWNNC system has been verified by some simulation and experimental results. The simulation and experimental results verify (1) a learning algorithm in a PID type form can achieve better tracking performance than the conventional learning algorithm; (2) the robust compensator can guarantee system stability and it does not result in any chattering phenomena; (3) the successful applications of the AFWNNC system to control a chaotic system and a DC motor.

## ACKNOWLEDGMENTS

The authors appreciate the partial financial support from the National Science Council of Republic of China under grant NSC 98-2221-E-216-040. The authors would like to express their gratitude to the reviewers for their valuable comments and suggestions.

**Table 1**  
Performance and Characteristic Comparison

controller	maximum tracking error (rad)	computational time (msec)	stability analysis	chattering phenomena	convergence speed
supervisory recurrent fuzzy neural network control (Lin and Hsu, 2004)	1.809	0.371	Yes	serious	slow
AFWNNC system with integral type adaptation law	4.227	0.392	Yes	none	slow
AFWNNC system with PID type adaptation law	0.615	0.396	Yes	none	fast

## REFERENCES

- [1] Billings, S. A. and Wei, H. L., "A New Class of Wavelet Networks for Nonlinear System Identification," *IEEE Trans. Neural Networks*, **16**(4), 862-874, 2005.
- [2] Chauhan, N., Ravi, V. and Karthik, C. D., "Differential Evolution Trained Wavelet Neural Networks: Application to Bankruptcy Prediction in Banks," *Expert Systems with Applications*, **36**(4), 7659-7665, 2009.
- [3] Damiano, A., Gatto, G. L., Marongiu, I. and Pisano, A., "Second-Order Sliding-Mode Control of DC Drives," *IEEE Trans. Ind. Electron.*, **51**(2), 364-373, 2004.
- [4] Golea, N., Golea, A. and Benmahammed, K., "Fuzzy Model Reference Adaptive Control," *IEEE Trans. Fuzzy Systems*, **10**(4), 436-444, 2002.
- [5] Ho, D., Zhang, P. A. and Xu, J., "Fuzzy Wavelet Networks for Function Learning," *IEEE Trans. Fuzzy Systems*, **9**(1), 200-211, 2001.

- [6] Hsu, C. F., "Intelligent Position Tracking Control for LCM Drive Using Stable Online Self-Constructing Recurrent Neural Network Controller with Bound Architecture," *Control Engineering Practice*, **17**(6), 714-722, 2009.
- [7] Hsu, C. F., Lin, C. M. and Lee, T. T., "Wavelet Adaptive Backstepping Control for A Class of Nonlinear Systems," *IEEE Trans. Neural Networks*, **17**(5), 1175-1183, 2006.
- [8] Hsu, C. F., Lin, C. M. and Chung, C. M., "Adaptive Position Tracking Control of a BLDC Motor Using a Recurrent Wavelet Neural Network," *International Journal of Computational Intelligence in Control*, **1**(2), 95-103, 2009.
- [9] Khan, M. A. S. K. and Rahman, M. A., "Implementation of A New Wavelet Controller for Interior Permanent-Magnet Motor Drives," *IEEE Trans. Ind. Appl.*, **44**(6), 1957-1965, 2008.
- [10] Lin, C. K., "Adaptive Critic Autopilot Design of Bank-To-Turn Missiles Using Fuzzy Basis Function Networks," *IEEE Trans. Systems Man Cybern. Part B*, **35**(2), 197-207, 2005.
- [11] Lin, C. K., "Nonsingular Terminal Sliding Mode Control of Robot Manipulators Using Fuzzy Wavelet Networks," *IEEE Trans. Fuzzy Systems*, **14**(6), 849-859, 2006.
- [12] Lin, C. K., " $H^\infty$  Reinforcement Learning Control of Robot Manipulators Using Fuzzy Wavelet Networks," *Fuzzy Sets and Systems*, **160**(12), 1765-1786, 2009.
- [13] Lin, C. M. and Hsu, C. F., "Supervisory Recurrent Fuzzy Neural Network Control of Wing Rock for Slender Delta Wings," *IEEE Trans. Fuzzy Systems*, **12**(5), 733-742, 2004.
- [14] Lin, C. M. and Peng, Y. F., "Adaptive CMAC-based Supervisory Control for Uncertain Nonlinear Systems," *IEEE Trans. Systems Man Cybern. Part B*, **34**(2), 1248-1260, 2004.
- [15] Lin, C. T. and Lee, C. S. G., *Neural Fuzzy Systems: A Neuro-Fuzzy Synergism to Intelligent Systems*, Englewood Cliffs, NJ: Prentice-Hall, 1996.
- [16] Lin, F. J., Wang, D. H., and Huang, P. K., "FPGA-based Fuzzy Sliding-Mode Control for A Linear Induction Motor Drive," *IEE Proc. Electr. Power Appl.*, **152**(5), 1137-1148, 2005.
- [17] Lin, F. J., Shieh, H. J. and Huang, P. K., "Adaptive Wavelet Neural Network Control with Hysteresis Estimation for Piezo-Positioning Mechanism," *IEEE Tran. Neural Networks*, **17**(2), 432-444, 2006.
- [18] Lin, F. J., Huang, P. K. and Chou, W. D., "Recurrent-Fuzzy-Neural-Network-Controlled Linear Induction Motor Servo Drive Using Genetic Algorithms," *IEEE Trans. Ind. Electr.*, **54** (3), 1449-1461, 2007.
- [19] Lin, F. J., Chen, S. Y. and Hung, Y. C., "FPGA-Based Recurrent Wavelet Neural Network Control System for Linear Ultrasonic Motor," *IET Electr. Power Appl.*, **3**(4), 298-312, 2009.
- [20] Nouri, K., Dhaouadi, R., Benhadj Braiek N., "Adaptive Control of a Nonlinear DC Motor Drive Using Recurrent Neural Networks," *Applied Soft Computing*, **8**(1), 371-382, 2008.
- [21] Peng, Y. F. and Hsu, C. F., "Identification-Based Chaos Control via Backstepping Design Using Self-Organizing Fuzzy Neural Networks," *Chaos, Solitons and Fractals*, **41**(3), 1377-1389, 2009.
- [22] Slotine, J. J. E. and Li, W. P., *Applied Nonlinear Control*, Englewood Cliffs, NJ: Prentice Hall, 1991.
- [23] Sousa, C. D., Hemerly, E. M. and Galvao, R. K. H., "Adaptive Control for Mobile Robot Using Wavelet Networks," *IEEE Trans. Systems Man Cybern. Part B*, **32**(4), 493-504, 2002.
- [24] Tang, Y., Sun, F. and Sun, Z., "Neural Network Control of Flexible-link Manipulators Using Sliding Mode," *Neurocomputing*, **70**(1), 288-295, 2006.
- [25] Wang, Z., Zhang, Y. and Fang, H., "Neural Adaptive Control for A Class of Nonlinear Systems with Unknown Deadzone," *Neural Comput. Appl.*, **17**(4), 339-345, 2008.
- [26] Zekri, M., Sadri, S. and Sheikholeslam, F., "Adaptive Fuzzy Wavelet Network Control Design for Nonlinear Systems," *Fuzzy Sets and Systems*, **159**(20), 2668-2695, 2008.
- [27] Zhang, Q., "Using Wavelet Network in Nonparametric Estimation," *IEEE Trans. Neural Networks*, **8**(2), 227-236, 1997.
- [28] [Online] <http://www.altera.com/>